

Inertia ratchets: A numerical study versus theory

B. Lindner,¹ L. Schimansky-Geier,¹ P. Reimann,² P. Hänggi,² and M. Nagaoka³

¹Humboldt-University at Berlin, Invalidenstrasse 110, D-10115 Berlin, Germany

²University of Augsburg, Memminger Strasse 6, D-86135 Augsburg, Germany

³Institute for Fundamental Chemistry, 34-4 Takano, Nishihiraki-cho, Sakyo-ku, Kyoto 606-8103, Japan

(Received 10 August 1998)

The colored (Ornstein-Uhlenbeck) noise-driven nonequilibrium dynamics of massive damped Brownian particles in a periodic but asymmetric potential (ratchet) is investigated. Our special focus is on the influence of inertia in the particle dynamics for the noise induced, directed current. By means of two approximation schemes (a unified colored noise approximation and a path-integral approach) and by numerical matrix-continued-fraction evaluations of the inherent, three-dimensional Fokker-Planck dynamics as well as by direct simulations of the stochastic differential equations we examine the dynamics at various inertial strengths. For the case of a large mass we find current reversal with respect to both a variation of the mass and of the noise-correlation time. Possibilities for efficient mass-sensitive scenarios for separation of particles are discussed. [S1063-651X(99)00802-8]

PACS number(s): 05.40.Ca, 82.20.Mj, 87.10.+e

I. INTRODUCTION

The constructive role of nonequilibrium noise and inherent equilibrium fluctuations, which—via the fluctuation-dissipation theorem—cause dissipation, can produce novel unexpected phenomena such as noise-induced directed current in periodic structures that lack reflection symmetry (ratchets), e.g. see the reviews [1,2], or anomalous amplification features for weak signals in thresholdlike systems (stochastic resonance) [3].

In recent years, a large variety of classical nonequilibrium ratchet models have been put forward that produce net transport in the presence of *unbiased* nonequilibrium forces. The interest in these models stems largely from their relevance for the operation of molecular motors [1,2,4] that drive intercellular transport processes. Likewise, recent active research has been fueled due to potential applications for novel technological devices that pump, trap or separate Brownian particles on periodic structures with period-length scales extending from nanoscopic to mesoscopic, up to macroscopic sizes [1].

To obtain directed transport with unbiased nonthermal fluctuations, the breaking of the reflection symmetry in periodic structures is no necessary prerequisite: Directed current occurs also with nonthermal, unbiased forces that exhibit nonvanishing *odd* numbered cumulant averages of order $n \geq 3$ (temporal asymmetry) [5]. A particular such realization appears by considering the (zero-frequency) *harmonic mixing signal* of two ac fields of angular frequencies Ω and 2Ω that drive overdamped classical transport in a (reflection-symmetric) cosine potential [6]. Noise-induced directed current in these systems has *implicitly* been observed experimentally (via the occurrence of a finite stop voltage) in one-dimensional organic conductors as early as in the late 1970s [7].

It should be noted, however, that the dynamics in ratchet structures with its inherent spatial asymmetry generally exhibits a richer complexity, such as the occurrence of a devil-staircase-like current quantization, multiple current reversals, and multip peaked current characteristics [1,2].

A particularly appealing feature of Brownian motors is their ability to separate particles of differing friction strength or mass [1]. It is this latter aspect of mass separation via *inertial correlation ratchets* [1] that is the focus of the present study. While the overwhelming part of ratchet dynamics has been studied in the overdamped limit, only a few prior studies considered the influence of inertial effects [8–11]. Reference [8] considered deterministically rocked inertial ratchets which are able to exhibit both regular and chaotic directed transport, as well as multiple current reversals.

The effect of quantum tunneling in combination with finite inertia has been addressed in Refs. [9] for rocked ratchets. Because inertial ratchets possess current reversals as a function of the mass of the particle [8–11], these ratchets are ideally suited to separate particles of differing masses [10,11], and thus allow for the conceptual operation of molecular shuttles [11], wherein an inertial Brownian carrier is able to move massive cargo back and forth along preassigned routes.

The operation of such an inertia ratchet was studied by Marchesoni [11] in the limit of weakly colored, unbiased nonthermal (Ornstein-Uhlenbeck) noise. In contrast, the role of moderate-to-large noise color—in the *presence* and in the absence of an external bias—was the objective of our investigation in Ref. [10]. In the following, we present a more detailed account of the phenomenon of mass separation in colored noise-driven inertia ratchets. In doing so, we present—apart from accurate numerical simulations of the underlying colored noise Langevin equation—precise matrix-continued-fraction results for the behavior of directed current. Our numerical results are compared vs. various theoretical predictions such as a generalized unified colored noise approximation scheme (UCNA) and an inertia-driven, colored noise path-integral approach that is valid at weak thermal noise.

To start, we present the model for the inertia ratchet, together with an appropriately chosen scaling to yield dimensionless variables with unit viscous friction strength.

II. MODEL FOR INERTIAL RATCHET DYNAMICS

We consider the dynamics of a Brownian particle in a periodic potential $U(x) = U(x + x_0)$ with broken spatial symmetry, known as the ratchet potential. Let x and v denote the space coordinate and velocity of the particle of mass m with η being the viscous friction strength. The stochastic ratchet dynamics then reads

$$\begin{aligned} \dot{x} &= v, \\ m\dot{v} &= -\eta v - U'(x) + F + y(t) + \sqrt{2D}\xi_1(t), \\ \dot{y} &= -\frac{y}{\tau} + \frac{\sqrt{2Q}}{\tau}\xi_2(t), \end{aligned} \quad (1)$$

$$\langle \xi_i(t)\xi_j(t') \rangle = \delta_{ij}\delta(t-t'),$$

$$\langle y(t)y(t') \rangle = \frac{Q}{\tau} \exp\left[-\frac{|t-t'|}{\tau}\right].$$

Here, the colored, unbiased noise $y(t)$ models stochastic nonequilibrium forces and the white noise $\xi_1(t)$ accounts for thermal fluctuations of strength D ($D = \eta k_B T$). Setting the colored noise source $y(t)$ equal to zero we recover an equilibrium system which cannot support finite, directed current. The perturbation $y(t)$ which drives the system out of equilibrium, is modeled here by the well-known Ornstein-Uhlenbeck Process (OUP) with an exponential correlation function— τ denotes its correlation time and Q the integrated intensity, often expressed by the ratio R of external and internal noise strength $Q = RD$. Moreover, we can include in our model an additional static bias F that is assumed to be zero if not stated otherwise.

The use of a scaling of the form

$$\begin{aligned} \tilde{t} &= t/t_0, & \tilde{x} &= x/x_0, & \tilde{v} &= v t_0/x_0, & \tilde{y} &= y V_0/x_0, \\ V(\tilde{x}) &= U(x)/V_0, & \tilde{F} &= x_0 F/V_0 \end{aligned}$$

leads to a dimensionless formulation of the dynamics in a potential V with $V(\tilde{x}) = V(\tilde{x} + 1)$. We choose $t_0 = \eta x_0^2/V_0$ to obtain a dimensionless friction coefficient equal to one. Then, the rescaled mass and noise parameters are given as

$$\mu = \frac{mV_0}{x_0^2\eta^2}, \quad \tilde{D} = \frac{D}{V_0\eta}, \quad \tilde{Q} = \frac{Q}{V_0\eta}, \quad \tilde{\tau} = \frac{\tau V_0}{\eta x_0^2}.$$

The new dimensionless dynamics reads

$$\begin{aligned} \dot{\tilde{x}} &= \tilde{v}, \\ \mu\dot{\tilde{v}} &= -\tilde{v} - V'(\tilde{x}) + \tilde{F} + \tilde{y}(\tilde{t}) + \sqrt{2\tilde{D}}\tilde{\xi}_1(\tilde{t}), \\ \dot{\tilde{y}} &= -\frac{\tilde{y}}{\tilde{\tau}} + \frac{\sqrt{2\tilde{Q}}}{\tilde{\tau}}\tilde{\xi}_2(\tilde{t}), \end{aligned} \quad (2)$$

where the tildes were omitted here and throughout later on.

The quantity of foremost interest is the mean velocity $\langle v \rangle$ or the steady state probability current of immersed Brownian

particles. We are interested in its dependences on the noise parameters, but particularly on the particle mass.

In view of the validity of equilibrium statistical mechanics the directed current assumes a zero value whenever

(1) $\tau \rightarrow 0$, i.e., the OUP becomes white, additive thermal equilibrium noise; (2) $\tau \rightarrow \infty$ or $Q \rightarrow 0$, implying a vanishing strength of the external nonequilibrium noise; (3) $D \rightarrow \infty$, in which limit the unbiased fluctuations dominate the potential forces, yielding zero current; and (4) $\mu \rightarrow \infty$, so that finite potential and fluctuating forces no longer are capable of moving particles. Furthermore, we remark that for $\mu \rightarrow 0$ one recovers the previously investigated overdamped situation in Ref. [12].

The Fokker-Planck-equation (FPE) for the probability density $P(x, v, y, t)$, corresponding to Eq. (2), i.e.,

$$\begin{aligned} \partial_t P &= -v \partial_x P + \partial_v \left(\frac{1}{\mu} v + \frac{V'(x) - y - F}{\mu} + \frac{D}{\mu^2} \partial_v \right) P \\ &+ \partial_y \left(\frac{y}{\tau} + \frac{Q}{\tau^2} \partial_y \right) P \end{aligned} \quad (3)$$

cannot be solved analytically even for the stationary case ($\partial_t P = 0$) since detailed balance is broken and the probability flow thus is not potential-like. Its dynamics (2), however, can be studied by means of analytical approximation schemes such as a unified colored noise approximation or a path-integral approach. Numerically, it can be investigated either by direct computer simulations of Eq. (2) or by applying the matrix-continued-fraction (MCF) method to the FPE (3). For our numerical evaluations we use throughout the specific ratchet potential

$$V(x) = -\frac{1}{2\pi} [\sin(2\pi x) + 0.25\sin(4\pi x)]. \quad (4)$$

In the following two sections we develop these two analytic approximation schemes for the inertia ratchet dynamics which will then be compared against precise numerical results.

III. UNIFIED COLORED NOISE APPROXIMATION

The unified colored noise approximation has originally been developed for overdamped stochastic dynamics driven by OUP [13]. Later refinements and generalizations have been put forward with Refs. [14,15]. It has proved to provide a good approximative description over wide parameter regimes for different situations and was applied already to colored noise-driven directed transport in Refs. [12,16].

The objective in the UCNA is to find an approximate Markovian description of a generally intractable non-Markovian dynamics [15]. First the non-Markovian dynamics is rewritten (if possible) as a higher-dimensional Markovian process introducing new variables for the noise. A nonlinear coordinate transformation to (approximately) decoupling stochastic variables is performed. In a second step, a separation of time scales for those new variables is established, thus admitting the adiabatic elimination of the ‘‘fast’’ ones. A Markovian description for the coordinate x only is achieved if this approach yields a single Langevin equation,

i.e., a first order differential equation with white noise sources.

Adapting this general line to Eq. (2) we find expressions for small correlation times τ and, simultaneously, for a strongly overdamped dynamics $\mu \rightarrow 0$. Within these restrictions, the following approximate Langevin equation (in Stratonovich interpretation) as Markovian approximation of Eq. (2) is derived [17]:

$$\dot{x} = \frac{1}{g(x)} [-V'(x) + F + \sqrt{2D(1+R)}\xi(t)], \quad (5)$$

where the state- and mass-dependent function $g(x)$ reads

$$g(x) = 1 + \frac{d}{dx} \frac{\tau R [V'(x) - F]}{(1+R)(1+\mu/\tau) + \tau V''(x)}. \quad (6)$$

For this Markovian approximation (5) the steady state probability current J can be calculated analytically following standard approaches [18]. With $\langle v \rangle = \langle \dot{x} \rangle = J$ we find

$$\langle \dot{x} \rangle = \frac{L(1+R)D[1 - e^{\Phi(1)/D}]}{\int_0^1 dx g(x) e^{-\Phi(x)/D} \int_x^{x+1} dy g(y) e^{\Phi(y)/D}}. \quad (7)$$

In this expression the effective potential

$$\Phi(x) = \int_0^x \frac{g(y)}{1+R} [V'(y) - F] dy \quad (8)$$

occurs. In the white noise limit $\tau \rightarrow 0$ it follows from Eq. (6) that $g(x) \rightarrow 1$. The current $\langle \dot{x} \rangle_{\tau=0}$ thus vanishes according to [6,7] if $F=0$, independent of the mass μ . Otherwise, that is, for $0 < \tau < \infty$, the current is generically nonzero for nonsymmetric potentials $V(x)$, even for $F=0$. The asymptotic behavior of Eq. (7) for small τ and zero load $F=0$ is obtained as

$$\langle \dot{x} \rangle = - \frac{\hat{\tau}^2 R}{A(0)(1+R)^2} \int_0^1 V'(y) V''(y)^2 dy, \quad \hat{\tau} = \frac{\tau}{1+\mu/\tau} \quad (9)$$

$$A(F) = \int_0^1 dx \int_x^{x+1} dy e^{[V(y) - V(x) + (x-y)F]/D(1+R)}. \quad (10)$$

Thus a τ^2 decay for moderately small τ is predicted, crossing over to a τ^4 decay for extremely small $\tau \ll \mu$. The μ dependence of the UCNA result (7) can be completely absorbed into the renormalized correlation time $\hat{\tau}$. For this reason the maximal value of $\langle \dot{x} \rangle$ with respect to τ is independent of μ .

IV. PATH-INTEGRAL APPROACH FOR INERTIA RATCHETS

In this section we aim at the calculation of the steady state current by use of path-integral methods.

As in quantum mechanics the corresponding reformulation of stochastic dynamics yields a compact representation [19,20]. In practice, however, the analytical evaluation of the resulting formal expressions is possible for weak thermal

noise D , only. Nevertheless, for situations where the potential barriers between adjacent metastable states renormalized by the colored noise are large compared to the strength of thermal fluctuations this approach has shown its powerful abilities.

Within the restriction of weak thermal noise the current of the Brownian particles can be approximated by a rate description

$$\langle \dot{x} \rangle = k_+ - k_-, \quad (11)$$

where $k_+(k_-)$ are noise-activated hopping rates to the next right (left) neighboring wells, respectively. We remember that $L=1$.

For small thermal noise D these rates approach an Arrhenius-like dependence $k_{\pm} = \zeta_{\pm} \exp(-\Delta\Phi_{\pm}/D)$. Therein $\Delta\Phi_{\pm}$ are ‘‘effective’’ potential barriers independent of D and ζ_{\pm} are rate prefactors.

In the case of small noise correlation time τ [21] we derive the explicit result

$$\begin{aligned} \Delta\Phi_{\pm}(\tau) &= \Delta\Phi_{\pm}^{(0)} + \Delta\Phi_{\pm}^{(1)}(\tau) \\ &= \frac{V(x^{\#}) - V(x_{\pm}) + (x_{\pm} - x^{\#})F}{1+R} \\ &\quad + \tau^2 \frac{R}{(1+R)^2} \int_{-\infty}^{\infty} \ddot{q}_{\pm}^2(t) dt, \end{aligned} \quad (12)$$

where $x^{\#}$ is the position of a local maximum of $V(x) - xF$ and x_+ and $x_- = x_+ - 1$ the location of the corresponding neighboring local minima to the right and left, respectively. The functions $q_{\pm}(t)$ are trajectories found from $\mu \ddot{q}_{\pm}(t) = -\dot{q}_{\pm}(t) - V'(q_{\pm}(t)) + F$ with initial conditions $q_{\pm}(t = -\infty) = x^{\#}$ and $\dot{q}_{\pm}(t = -\infty) = 0$ and ending in one of the possible minima as $t \rightarrow \infty$. We label $q_{\pm}(t = \infty) = x_{\pm}$.

In the prefactor ζ_{\pm} we restrict ourselves to the zeroth order approximation $\zeta(\tau) \approx \zeta(\tau=0)$ with the effective noise $D(1+R)$. A closer inspection involving detailed-balance arguments, as well as explicit perturbation calculations [22], has shown that the identity $\zeta_+(\tau=0) = \zeta_-(\tau=0)$ should hold true in the spatial diffusion regime whenever the concept of an escape rate makes sense. We thus infer that

$$\langle \dot{x} \rangle = B [e^{-\Delta\Phi_+^{(1)}/D} - e^{-\{\Delta\Phi_-^{(1)} + LF/(1+R)\}/D}], \quad (13)$$

where $B = k_+(\tau=0)$. Next, we make use of an observation that can be inferred from Eq. (7), namely, that the current for vanishing τ is essentially independent of μ if $F \neq 0$. This independence of the mass is inherited by the factor B . By setting $\mu=0$ we obtain approximately

$$B = \frac{(1+R)D}{A(F)}, \quad (14)$$

where $A(F)$ is defined in Eq. (10). For zero load $F=0$ and expanding the exponential in Eq. (13) one finds to leading order in τ

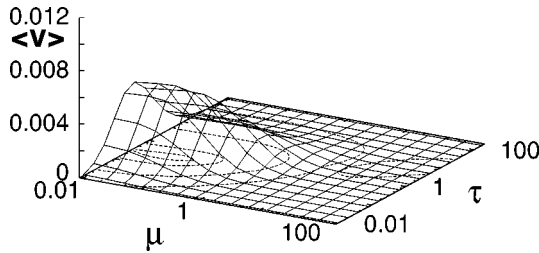


FIG. 1. Mean velocity $\langle v \rangle$ vs correlation time τ and mass μ . Negative velocity appearing in the underdamped regime is indicated only by contour lines, because its order of magnitude is much smaller than in the damped case. The parameters chosen are $D=0.1$, $Q=0.05$, here $R < 1$.

$$\langle \dot{x} \rangle = - \frac{\tau^2 R}{A(0)(1+R)} \int_{-\infty}^{\infty} [\ddot{q}_+(t)^2 - \ddot{q}_-(t)^2] dt. \quad (15)$$

We want to point out that $\Delta\Phi_+^{(1)} - \Delta\Phi_-^{(1)}$ can change its sign depending on μ . In fact formula (13) predicts a reversal of the current direction in the underdamped regime ($\mu \gg 1$), as is shown in Fig. 3. Note, however, that this prediction is qualitative only: The reversal occurs in the energy-diffusion limited regime, where our result (13) fails quantitatively. Here besides site-to-site hopping events long excursions over multiple barriers appear that are not taken into account by Eq. (11). Nevertheless, their occurrences are given in good approximation by the rates k_{\pm} and, therefore, depend on the asymmetry of the ratchet potential. Hence, the difference between forward and backward rates serves as a good indicator for an actual reversal of current as is confirmed by the numerical analysis, later on.

V. MATRIX-CONTINUED-FRACTION ANALYSIS

To cover a large range of parameters we solved Eq. (3) numerically by use of the method of matrix-continued fractions. We developed the steady state density $P(x, v, y)$ in a (finite) set of proper eigenfunctions [23]. We used Hermite functions in v and y , and Fourier modes in the coordinate x . The corresponding recursion relations between matrices has been solved numerically by applying Risken's method [24].

The dependence on mass μ and correlation time τ of noise-induced currents calculated for two different values of Q are depicted in Figs. 1 and 2. We have chosen the intensity of the colored noise Q smaller and larger than the thermal noise D , see Fig. 1 and Fig. 2, respectively. As mentioned in Sec. II the current disappears for large mass as well as for vanishing and large τ . For small μ (overdamped regime) the

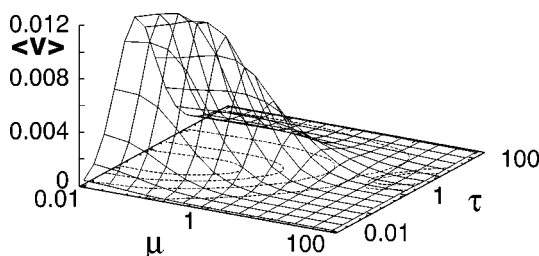


FIG. 2. Mean velocity $\langle v \rangle$ vs correlation time τ and mass μ . The parameters chosen are $Q=0.12$, here $R > 1$, the absolute value of negative velocity, is greater than in Fig. 1.

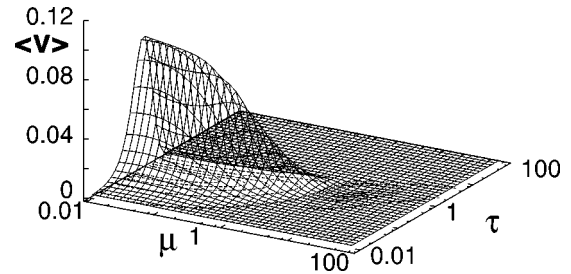


FIG. 3. Mean velocity $\langle v \rangle$ vs correlation time τ and mass μ . Path-integral approximation (13) for $D=0.1$ and $Q=0.12$.

current converges to the results from [12]. Predictions of the path-integral approach [Eq. (13)] are presented in Fig. 3.

The finite inertia causes a complex behavior of the current behavior as can be deduced from all the figures. Starting with small values of μ we observe for a certain range of τ a novel unexpected increase of the current with respect to μ (Figs. 1 and 2). Thus a global maximum with respect to both μ and τ appears for finite mass, and hence finite inertia may enhance the value of the mean velocity of Brownian particles in ratchets.

Further increasing inertia (above $\mu \approx 0.1$) yields a rapid decrease of the current. Thereby for a given μ , the maximum with respect to τ shifts toward larger values which agrees with the predictions of the UCNA and of the path-integral approximation. This drop of the current is expected since the fluctuational and potential forces have a weaker effect on a larger mass. Hence, the mean velocity decreases. The shift of the maximum results from a slowing down of the particle motion if increasing the mass. This can be compensated by a larger correlation time τ .

A second novelty is found in the strongly underdamped case at arbitrary R , namely a negative velocity appears for moderate τ . The MCF analysis shows a rich behavior. First, for moderate values of μ we found a double reversal of the velocity direction for increasing values of the correlation time (Fig. 4). Negative currents are observed for moderate correlation times only. For larger μ the current exhibits a single reversal. Now it is still positive for large τ (Fig. 5).

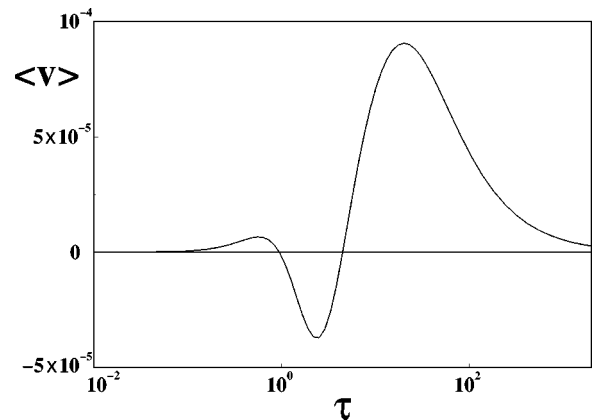


FIG. 4. Mean velocity $\langle v \rangle$ vs correlation time τ for the parameters $D=0.1$, $Q=0.05$, $\mu=20.0$.

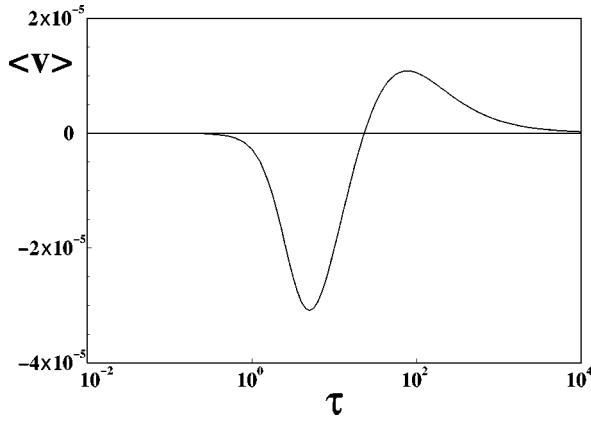


FIG. 5. Mean velocity $\langle v \rangle$ vs correlation time τ for the parameters $D=0.1$, $Q=0.05$, $\mu=60.0$.

We underline that the absolute values of the reversed currents are rather small compared to the maximal current for small masses.

Let us compare our numerical results with the predictions of the path-integral approach. Generally, as depicted in the figures, this method overestimates the current by one order of magnitude, but it captures qualitatively the interesting effects found in the MCF calculations. The global maximum with growing mass does not appear in Fig. 3. This is apparently due to the approximation of small τ we made. In the region of moderate mass the path-integral analysis correctly predicts the shift and the decrease of the current maximum. Most interestingly, the path-integral approach predicts a current reversal as a function of the mass μ ; but it predicts a negative current for all τ values above a certain value μ .

The increase of Q in the examples considered, i.e., a change from $R < 1$ to $R > 1$, leads in general to an amplification of the positive and even of the negative current. We want to stress that our observed reversal is different from the one predicted in Ref. [11]. In Figs. 1 and 2 current reversals occur for sufficiently large μ without a restriction on the ratio $R=Q/D$. Conditions for the current reversal in [11] would imply $\mu < 1$ and $R < 1$.

The value of R can also be changed via varying D while keeping Q fixed. This influence of the thermal fluctuation is illustrated in Figs. 6 and 7. In the case of positive velocities we obtain a nonmonotonous behavior, the ratchet current

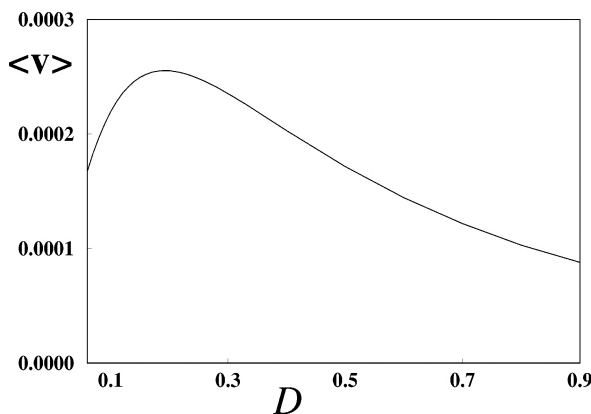


FIG. 6. Mean velocity $\langle v \rangle$ vs noise intensity D . Parameters: $\tau=0.5$, $Q=0.1$, $\mu=5.0$.

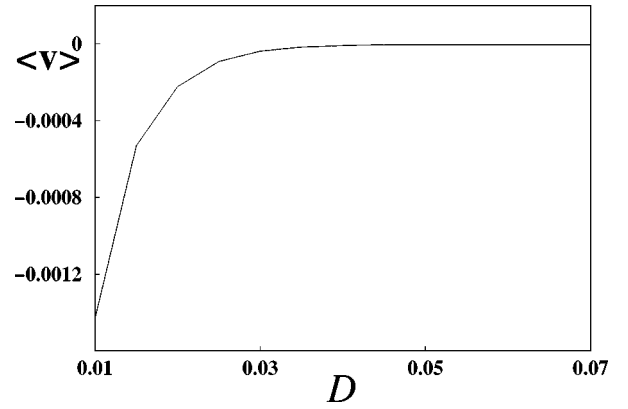


FIG. 7. Mean velocity $\langle v \rangle$ vs noise intensity D . Parameters: $\tau=3.5$, $Q=0.035$, $\mu=12.5$.

reaches a maximum at finite temperature. White noise can enhance the induced transport which has already been demonstrated in the overdamped case [12]. In the underdamped case, for occurring negative currents, this could not be verified. The absolute value of the current decreases monotonically with increasing diffusion D (cf. Fig. 7). Moreover, white noise seems rather to destroy the induced reversal of current than to amplify it.

VI. COMPARISON WITH LANGEVIN SIMULATIONS

The dynamics of Brownian particles in ratchet potentials can be investigated also via a second numerical approach. Simulations of the Langevin equations (1) allow the investigation of trajectories and will later provide insight into the mechanism of the current reversal. Here we should mention the nearly exact agreement of the mean values as obtained from the simulations with the results of the MCF calculations.

We have implemented the Fox algorithm [17,25], which is a rather fast method for simulating processes driven by the OUP. For each set of parameter values the stochastic dynamics was integrated over 10^7 time steps $\Delta t=10^{-2}$ and the time-averaged velocity was determined from $[x(T) - x(0)]/T$. This time averaging was repeated 20 times to obtain the mean current in sufficiently high accuracy (less than 5% for $\tau > 0.1$). The relative numerical error increases both with increasing μ in Eq. (1) and decreasing τ and we

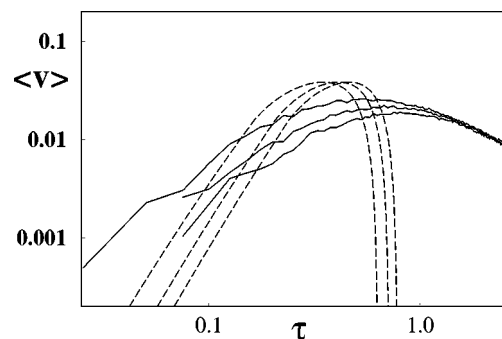


FIG. 8. Mean velocity $\langle v \rangle$ vs correlation time τ . Numerical simulations (solid) compared to UCNA. The parameters used are $D=0.05$, $Q=RD=0.25$, $F=0$. The inertia values used are $\mu=0.125$, $\mu=0.25$, and $\mu=0.375$.

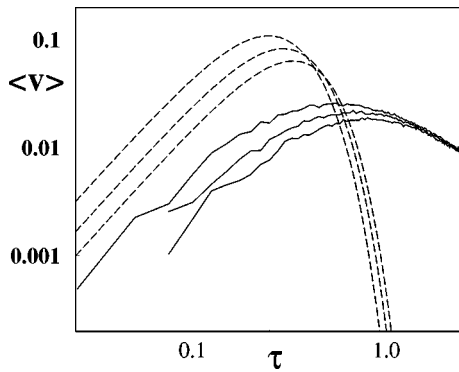


FIG. 9. Mean velocity $\langle v \rangle$ vs correlation time τ . Numerical simulations (solid) compared to path integrals. The parameters used are $D=0.05$, $Q=RD=0.25$, $F=0$. The inertia values used are $\mu=0.125$, $\mu=0.25$, and $\mu=0.375$.

could not reach the deep asymptotic regime $\tau \rightarrow 0$.

The comparison for moderate-to-small μ and moderate-to-small τ of the UCNA with the simulations is depicted in Fig. 8 for different μ values. The maximum of the UCNA shifts towards larger τ with increasing mass, in agreement with the simulations and the MCF results. The simultaneous decrease of the maximal value of the current is not predicted by the UCNA.

A comparison between the path-integral prediction (13), (14) and the numerical simulations is shown in Fig. 9. The agreement is satisfactory up to about $\tau=0.5$, apart from its absolute value which is better estimated by the UCNA. The shift with respect to τ and the decrease of the maximum with increasing inertia μ —as already mentioned above—are well described. In particular, the asymptotics in Eq. (15) seems to agree better with the numerics than that from the UCNA approach (10).

The MCF curves and the results of the simulations (Fig. 10) nearly converge. Both dependences, i.e., the shift of the maximal current to larger values of τ as well as the decrease of the current with increasing μ , are correctly rendered by the MCF. Apart from the different computing time of the simulation and the MCF data (the simulations require two orders of magnitude larger CPU times), the MCF results even achieve a higher accuracy for small τ than the simulations.

Also the current reversal in the underdamped case was

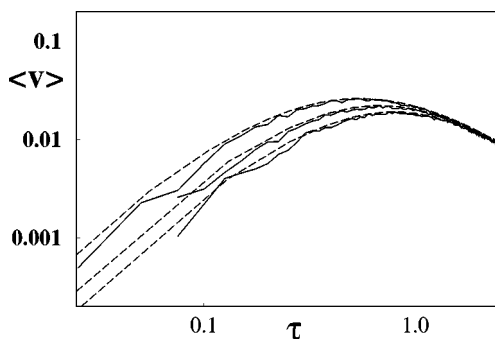


FIG. 10. Mean velocity $\langle v \rangle$ vs correlation time τ . Numerical simulations (solid) compared to MCF. The parameters used are $D=0.05$, $Q=RD=0.25$, $F=0$. The inertia values used are $\mu=0.125$, $\mu=0.25$, and $\mu=0.375$.

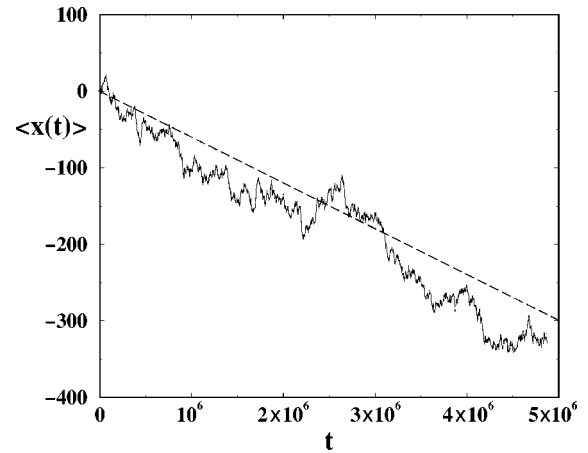


FIG. 11. The averaged motion of 20 particles moving in opposite direction (regime of current reversal). The dashed line depicts the MCF result for the average motion. The chosen parameters are $D=0.1$, $Q=0.1$, $\mu=51.2$, $\tau=3.58$.

verified by simulations (Fig. 11). Apart from superimposed stochastic deviations the averaged position of 20 particles vs. time exhibits the directed motion predicted by the MCF (dashed line). A time span of two individual trajectories demonstrates the effect of strong inertia (Fig. 12): For sufficiently large correlation times τ the accelerated particles may achieve a large amount of kinetic energy, allowing them to pass over a number of intermediate barriers (notice here that $L=1$) before they stop again in a well. In the underdamped regime one can generally distinguish between “running states” and “locking states.” In the second state the particles are bound in one of the minima, whereas in the first they cover distances over several periods in both directions. But the reversed motion results neither from a relevant difference of the velocities to the right and to the left, nor from a difference of the back transition rates into the “locked solution.” In the simulations we found a distinct difference of rates for transitions from the locked state into the left-, or right-running state, which originates from the asymmetry of the potential. This is the reason why the path-integral approach, which is based on jump rates k_+ and k_- , does indeed exhibit the current reversal.

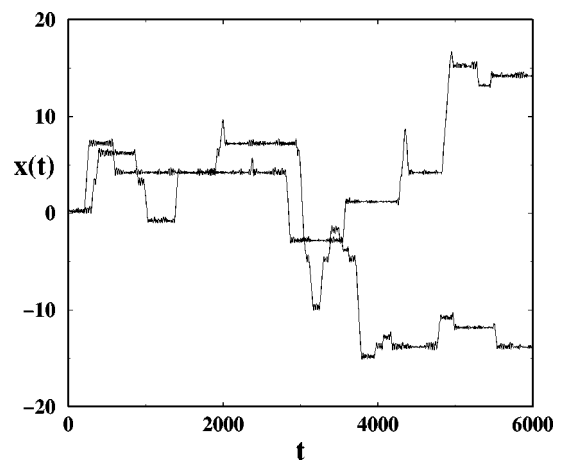


FIG. 12. Two individual trajectories $x(t)$ are shown. The parameters chosen are $D=0.1$, $Q=0.1$, $\mu=51.2$, $\tau=3.58$.

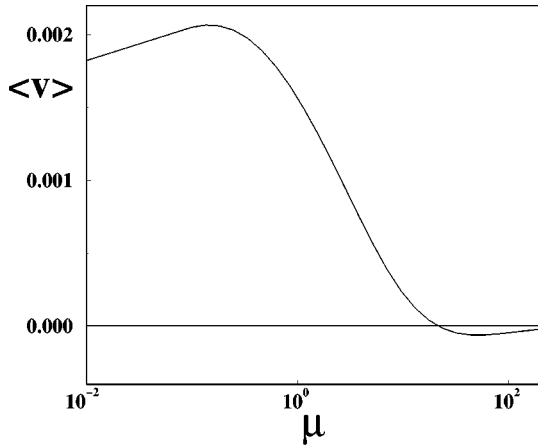


FIG. 13. Velocity reversal in the underdamped case with respect to mass μ , evaluated with the MCF method. The parameters are $D=0.1$, $Q=0.1$, $\tau=5.0$.

VII. MASS SEPARATION

Besides a size-dependent separation due to different friction constants of the particles, a separation due to mass difference constitutes a new and independent mechanism [11]. We next discuss what possibilities for this kind of particle separation result from our study.

The first situation would be that the particles move in different regimes, overdamped and underdamped, which assumes situations with large differences in μ . Then—as discussed above—there exists a certain set of noise parameters leading to different directions of the particles, as illustrated in Fig. 13.

Next, let us consider massive particles with non-negligible inertia (moderate μ). As shown before, we obtained a displacement of the maximal current for increasing values of the mass μ . This shift can be used in effect for the purpose of separating mesoscopic particles with different masses. Adding a constant force against the preferred direction of the ratchet, a current reversal will emerge in a finite region of τ . Beginning from a first value τ_1 until a second value τ_2 the noise-induced current overcompensates the ac-

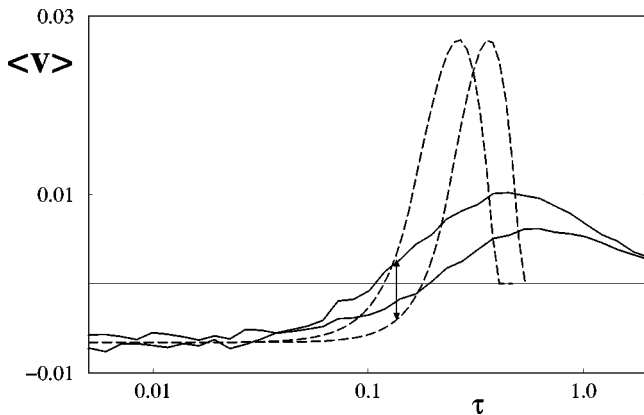


FIG. 14. The results for the UCNA (dashed) compared against simulations (solid lines). Parameters: $D=0.05$, $Q=0.125$, $F=-0.01$, for $\mu=0.125$ (curve, that reaches maximal current for smaller τ), and $\mu=0.375$, respectively. The arrow indicates an optimal τ value allowing for effective mass separation.

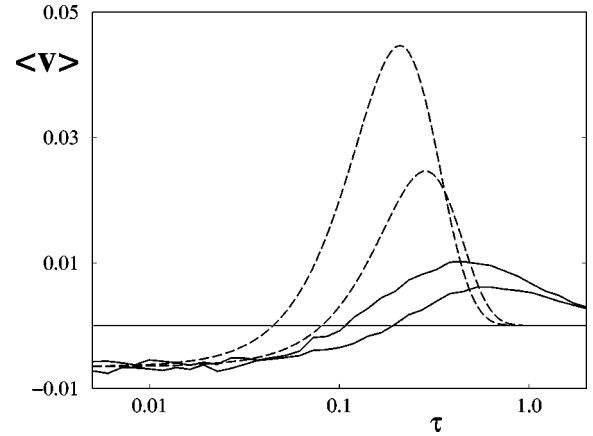


FIG. 15. The results for the path-integral approximation (dashed) compared against simulations (solid lines). Parameters: $D=0.05$, $Q=0.125$, $F=-0.01$, for $\mu=0.125$ (curve, that reaches maximal current for smaller τ), and $\mu=0.375$, respectively.

tion of the (small) load force. Both values, τ_1 and τ_2 , depend on the mass of the particle. Hence for two different values of the mass nonoverlapping regions of current reversals are possible. This in turn yields the desired separation of the two species of particles.

Results of simulations and of the estimations from the UCNA and the path integral approach are depicted in Figs. 14 and 15. For a specific range of τ the particles have different signs of velocity, and hence exhibit flow on the average in different directions. An increase of the differences of the masses would strengthen the speed of separation and enlarge the region of allowed correlation times.

VIII. CONCLUSIONS

We have presented analytical and exact numerical results as well as computer simulations for the dynamics of a massive Brownian particle in a ratchet potential subjected to external colored and internal white fluctuations. We could demonstrate that finite inertia can enhance the noise-induced transport and that for this transport there exists an optimal temperature of the embedding bath. In the underdamped case we could detect a current reversal, which has been predicted by the path-integral approach. The possibility of separating particles with respect to their masses in the regimes of moderate and strong inertia was demonstrated. It is conceivable that this novel separation mechanism could be of use in technical applications, working at a mesoscopic level.

ACKNOWLEDGMENTS

We would like to thank Roland Bartussek for his advice and help with the MCF calculations. This work has been supported by the Deutsche Forschungsgemeinschaft via Sachbeihilfe (Grant Nos. HA1517/13-2, SCHI 354/5-1, GRK 268, and 283), and the Germany-Japan program with the Japan Society for the Promotion of Science (JSPS), where a part of this work was completed while visiting the Institute for Fundamental Chemistry in Kyoto.

- [1] P. Hänggi and R. Bartussek, *Nonlinear Physics of Complex Systems—Current Status and Future Trends* (Springer, Berlin, 1996).
- [2] C. R. Doering, *Nuovo Cimento D* **17**, 685 (1995); R. D. Astumian, *Science* **276**, 917 (1997); F. Jülicher, A. Ajdari, and J. Prost, *Rev. Mod. Phys.* **69**, 1269 (1997).
- [3] P. Jung, *Phys. Rep.* **234**, 175 (1993); L. Gammaitoni, P. Hänggi, P. Jung, and F. Marchesoni, *Rev. Mod. Phys.* **70**, 223 (1997).
- [4] M. Magnasco, *Phys. Rev. Lett.* **71**, 1477 (1993).
- [5] C. Van den Broeck and P. Hänggi, *Phys. Rev. A* **30**, 2730 (1984); M. Milonas and M. Dykman, *Phys. Lett. A* **185**, 65 (1994); J. Luczka, R. Bartussek, and P. Hänggi, *Europhys. Lett.* **31**, 431 (1995); P. Hänggi, R. Bartussek, P. Talkner, and J. Luczka, *ibid.* **35**, 315 (1996); D. R. Chialvo, M. I. Dykman, and M. M. Milonas, *Phys. Rev. Lett.* **78**, 1605 (1997); I. Zapata, J. Luczka, F. Sols, and P. Hänggi, *ibid.* **80**, 829 (1998).
- [6] W. Wonneberger and H.-J. Breymayer, *Z. Phys. B* **56**, 241 (1984); H.-J. Breymayer, H. Risken, H. D. Vollmer, and W. Wonneberger, *Appl. Phys. B: Photophys. Laser Chem.* **28**, 335 (1982). Note, however, that noise-induced, directed current at zero external bias (i.e., rectification features) was not considered in these early works.
- [7] K. Seeger and W. Maurer, *Solid State Commun.* **27**, 603 (1978).
- [8] P. Jung, J. G. Kissner, and P. Hänggi, *Phys. Rev. Lett.* **76**, 3436 (1996).
- [9] P. Reimann, M. Grifoni, and P. Hänggi, *Phys. Rev. Lett.* **79**, 10 (1997); P. Reimann and P. Hänggi, *Chaos* **8**, 629 (1998).
- [10] B. Lindner, L. Schimansky-Geier, P. Reimann, and P. Hänggi, in *Applied Nonlinear Dynamics and Stochastic Systems near the Millennium*, edited by James B. Kadtko and Adi Bulsara, AIP Conf. Proc. No. 411, (AIP, Woodbury, NY, 1997), p. 309.
- [11] F. Marchesoni, *Phys. Lett. A* **237**, 126 (1998).
- [12] R. Bartussek, P. Reimann, and P. Hänggi, *Phys. Rev. Lett.* **76**, 1166 (1996).
- [13] P. Jung and P. Hänggi, *Phys. Rev. A* **35**, 4464 (1987).
- [14] L. H'walisz, P. Jung, P. Hänggi, P. Talkner, and L. Schimansky-Geier, *Z. Phys. B* **77**, 471 (1989); L. Schimansky-Geier and Ch. Zülicke, *ibid.* **79**, 451 (1990); A. J. R. Madureira, P. Hänggi, V. Buonomano, and W. A. Rodrigues, Jr., *Phys. Rev. E* **51**, 3849 (1995); R. Bartussek, A. J. R. Madureira, and P. Hänggi, *ibid.* **52**, 2149 (1995).
- [15] P. Hänggi and P. Jung, *Adv. Chem. Phys.* **89**, 239 (1995).
- [16] R. Bartussek, P. Hänggi, B. Lindner, and L. Schimansky-Geier, *Phys. Rev. D* **109**, 17 (1997).
- [17] B. Lindner, Master thesis, Humboldt University at Berlin, 1996.
- [18] R. L. Stratonovich, *Topics in the Theory of Random Noise* (Gordon and Breach, New York, 1967), Vol. 2.
- [19] R. Graham and T. Tel, *Phys. Rev. A* **31**, 1109 (1985); P. Hänggi, *Z. Phys. B* **75**, 275 (1989); H. S. Wio, P. Colet, M. San Miguel, L. Pesquera, and M. A. Rodriguez, *Phys. Rev. A* **40**, 7312 (1989).
- [20] S. B. J. Eichcomb and A. J. McKane, *Phys. Rev. E* **51**, 2974 (1995).
- [21] R. Reimann, *Phys. Rev. E* **52**, 1579 (1995); K. M. Rattray and A. J. McKane, *J. Phys. A* **24**, 1215 (1991).
- [22] E. Pollak and P. Talker, *Phys. Rev. E* **47**, 922 (1993).
- [23] R. Bartussek, in *Stochastic Dynamics*, edited by L. Schimansky-Geier and T. Pöschel, *Lecture Notes in Physics* Vol. 484 (Springer, Berlin, 1997), pp. 69–80.
- [24] H. Risken, *The Fokker-Planck Equation* (Springer, Berlin, 1984).
- [25] R. F. Fox, I. R. Gatland, R. Roy, and G. Vemuri, *Phys. Rev. A* **38**, 5938 (1988).